Reduced-Complexity Transmit/Receive-Diversity Systems

Andreas F. Molisch, *Senior Member, IEEE*, Moe Z. Win, *Senior Member, IEEE*, and Jack H. Winters, *Fellow, IEEE*

***Abstract*—We consider wireless systems with transmit and receive diversity. For reduction of complexity, we propose to use hybrid selection/maximal-ratio transmission at one link end, choosing L out of N antennas. We analyze the performance of such systems, giving analytical bounds and comparing them with computer simulations. Outage probability, symbol error probability, and capacity are shown. We demonstrate that in typical cases, a small number of used antennas L is sufficient to achieve considerable performance gains. We also analyze the influence of the number of antennas at the other link end, of fading correlation, and of channel estimation errors. The simulation results confirm that the proposed scheme is effective in a variety of environments.**

***Index Terms*—Antenna selection, channel estimation, diversity, MIMO.**

I. Introduction

SYSTEMS with multiple antennas at both transmitter and receiver have received considerable attention in recent years [1], [2]. One approach to utilizing multiple transmit antennas is to transmit different data streams from each antenna; these streams can be separated at the receiver side by using signal processing techniques such as the so-called BLAST schemes [3], [4]. However, these approaches cannot be used with existing standards as the requirement of backward-compatibility is not fulfilled.

An alternative way for exploiting multiple antenna elements at transmitter and receiver is the use of transmit and receive diversity purely for link-quality improvement, exploiting the diversity effect. Transmit diversity schemes were first proposed in [5] and [6] for the enhancement of transmission quality in mobile radio systems. In such a system, the signals supplied to the different transmit antennas are weighted replicas of a single bit stream (which might be coded or uncoded). The ideal weights can be determined by matching them to the channel, resulting in maximal-ratio transmission (MRT) [7]. Similarly, at the receiver, "standard" maximal-ratio combining (MRC) can be employed, using linear combinations of the signals obtained at the different receive antennas. It has been shown that with N_{t} transmit and N_{r} receive antennas, a diversity degree of $N_{\mathrm{t}}N_{\mathrm{r}}$ can be achieved [8]. Note that since it employs no special type of coding, any standard (single-antenna) receiver can detect the transmitted signal (albeit with a smaller diversity degree and thus reduced quality).

The main disadvantage of MRT (MRC) is the fact that it requires $N_{\mathrm{t}}(N_{\mathrm{r}})$ complete RF chains. There are numerous situations where this high degree of hardware complexity is undesirable—this is especially important for the mobile station (MS). On the other hand, a simple (one out of N) selection diversity gives considerably worse results. A compromise between these two possibilities is hybrid selection/maximum-ratio combining (H-S/MRC[1] [9]–[13]), where the best L out of N antennas are selected, and then combined, thus reducing the number of required RF chains to L.[2]

In this paper, we consider a transmit/receive diversity system where the transmitter uses hybrid selection/maximal-ratio transmission (H-S/MRT), whereas the receiver uses MRC. We will analyze the performance of such a system in terms of signal-to-noise ratio (SNR), symbol error probability (SEP), and capacity. In Section II, we describe the model for the system and the wireless channel. Next, we derive bounds for the system performance in terms of SNR, capacity, and (uncoded) bit error probability. For these theoretical considerations, we use some idealizations. In the next section, we present results both from the theoretical analysis and from Monte Carlo simulations. Those simulations are used to show the validity of our theory, as well as for investigating the influence of nonidealities in the system. A summary wraps up the paper.

II. System and Channel Model

Fig. 1 shows the generic system that we are considering. A bit stream is sent through an encoder and a modulator. A multiplexer switches the modulated signals to the best L_{t} out of N_{t} available antenna branches. For each selected branch, the signal is multiplied by a complex coefficient w whose actual value depends on the current channel realization. In a real system, the

Manuscript received December 15, 2002; revised May 2, 2003. This work was supported in part by the Austrian Ministry of Education and Science, TU Wien, Oesterreichische Forschungsgemeinschaft, and an INGVAR grant of the Swedish Strategic Research Foundation. This paper was presented in part at the IEEE International Conference on Communications, Helsinki, Finland, June 2001, and in part at the International Symposium on Wireless Personal Multimedia Communications, Honolulu, HI, October 2002. The associate editor coordinating the review of this paper and approving it for publication was Dr. Michael P. Fitz.

A. F. Molisch was with AT&T Labs—Research, Middletown, NJ 07848 USA. He is now with Mitsubishi Electric Research Labs, Cambridge, MA 02139 USA, and also with Lund University, Lund, Sweden (e-mail: Andreas.Molisch@ieee.org).

M. Z. Win was with AT&T Labs—Research, Middletown, NJ 07848 USA. He is now with the Laboratory for Information and Decision Systems (LIDS), Massachusets Institute of Technology, Cambridge, MA 02118 USA (e-mail: moewin@mit.edu).

J. H. Winters was with the AT&T Labs—Research, Middletown, NJ 07748 USA. He is now with Jack Winters Communications LLC, Middletown, NJ 07848 USA (e-mail: jack@jackwinters.com).

Digital Object Identifier 10.1109/TSP.2003.818211

[1]H-S/MRC in the following can denote either the transmission or the reception case.

[2]The case that one link end uses MRC, while the other uses pure selection combining, i.e., selecting only a single antenna out of N available, is treated in [14].

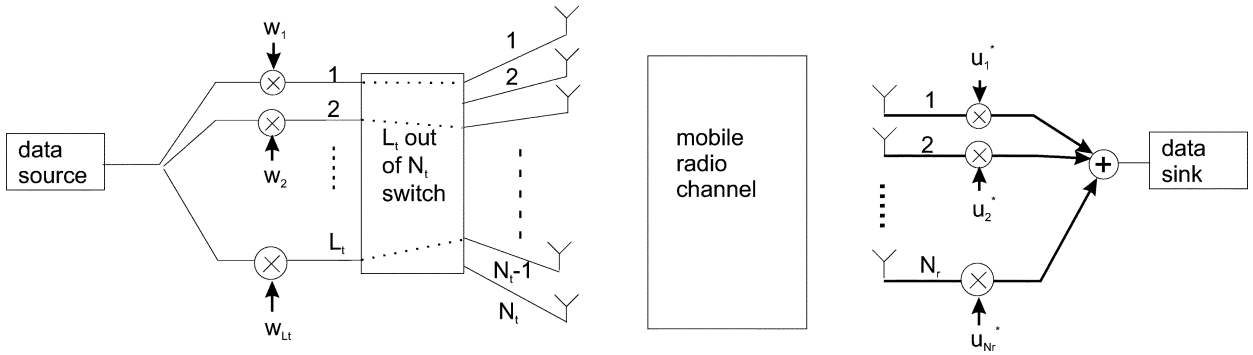

Fig. 1. System model.

signals are subsequently upconverted to passband, amplified by a power amplifier, and filtered. For our model, we omit these stages, as well as their corresponding stages at the receiver, and treat the whole problem in equivalent baseband. Note, however, that exactly these stages are the most expensive and make the use of reduced-complexity systems desirable.

Next, the signal is sent over a quasistatic flat-fading channel. We denote the $N_{\mathrm{r}} \times N_{\mathrm{t}}$ matrix of the channel as H. The output of the channel is polluted by additive white Gaussian noise, which is assumed to be independent at all receiver antenna elements. The received signals are multiplied by complex weights u^* at all antenna elements (where superscript * denotes complex conjugation) and combined before passing a decoder/detector.

For the theoretical analysis in Section III, we make some additional simplifying assumptions:

i) The fading at the different antenna elements is assumed to be independent, identically distributed Rayleigh fading. The h_{ij} are modeled as independent identically distributed zero-mean, circularly symmetric complex Gaussian random variables with unit variance, i.e., the real and imaginary part each have variance 1/2. Consequently, the power carried by each transmission channel (h_{ij}) is chi-square distributed with 2 degrees of freedom. Our methodology is also applicable for Nakagami fading with integer m-parameter. However, we note that independent Nakagami fading with $m > 1$ rarely occurs in practice, as a large Nakagami parameter indicates line-of-sight, which induces correlation between the fading. The influence of correlation on the achievable capacity will be discussed in Section IV.

ii) The fading is assumed to be frequency flat. This is fulfilled if the coherence bandwidth of the channel is significantly larger than the system bandwidth.

iii) We assume that both transmitter and receiver have perfect knowledge of the channel. This is, of course, an idealization that can only be approximated even in slowly fading channels. The receiver can obtain its channel knowledge either from the demodulation of training sequences (in TDMA systems) or pilot tones (for CDMA or OFDM systems). Alternatively, the use of blind channel estimation methods is a viable approach but results in a higher complexity. The transmitter can obtain the channel information either by feedback from the receiver or from the antenna weights generated during reception on the reverse link. Note that the latter approach requires the duplex frequency separation to be much smaller than the coherence bandwidth (in a frequency division duplexing scheme) or the duplex time to be much smaller than the coherence time of the channel (in a time-division duplexing scheme). In practical systems, the former condition is usually violated, whereas the latter condition is fulfilled. For example, cordless systems like digital enhanced cordless telecommunications (DECT) [15], the personal handyphone system (PHS) [16], or the personal access communications system (PACS) [17] exhibit duplex times of a few milliseconds—considerably less than the typical coherence time, which is related to the inverse of the maximum Doppler frequency at pedestrian movement speeds. The influence of wrong antenna selection due to channel estimation errors will be discussed in Section IV.

III. Computation of Performance

A. Channel Statistics and Optimum Weights

We first determine the optimum antenna weights and the statistics of the fading channel. The easiest way for deriving the optimum weights is a singular value decomposition of the channel matrix $H = U\Lambda W^*$, where Λ is a diagonal matrix containing the singular values, and U and W^* are unitary matrices composed of the left and right singular vectors, respectively [18]. The optimum transmit weight vector $\overrightarrow{w}$ and optimum receive weight vector $\overrightarrow{u^*}$, respectively, can now be shown to be the right and left conjugated singular vectors belonging to the largest singular value [8]. The effective SNR is given by the square of this singular value, i.e., the eigenvalue of $HH^\dagger$, where superscript † denotes Hermitian transpose. Note that this derivation assumes the use of all available antennas at both transmitters and receivers.

Our goal here is to determine the performance when only a subset of the antennas are used. For this, we have to define a set of matrices $\widetilde{H}$, where $\widetilde{H}$ is created by striking $N_{\mathrm{t}} - L_{\mathrm{t}}$ columns from H, and $S(\widetilde{H})$ denotes the set of all possible $\widetilde{H}$, whose cardinality is $\binom{N_{\mathrm{t}}}{L_{\mathrm{t}}}$. The achievable SNR of the reduced-complexity system is now

$$\gamma_{\mathrm{H-S/MRC}} = \max_{S(\widetilde{H})} \left(\max_i \left(\widetilde{\lambda}_i^2 \right) \right) \tag{1}$$

where the $\widetilde{\lambda}_i$'s are the singular values of $\widetilde{H}$.

An analytical solution $\mathrm{SNR}_{\mathrm{H-S/MRC}}$ does not seem to be easily obtainable. However, we can derive upper and lower bounds. We start out by stating that

$$\frac{1}{\min(L_{\mathrm{t}}, N_{\mathrm{r}})} \sum_i \widetilde{\lambda}_i^2 \leq \max_i \left(\widetilde{\lambda}_i^2\right) \leq \sum_i \widetilde{\lambda}_i^2 \tag{2}$$

i.e., the achievable SNR for a certain modified channel matrix $\widetilde{H}$ is lower bounded by the *average* of the nonzero eigenvalues and upper bounded by the *sum* of the nonzero eigenvalues of $\widetilde{H}$. We thus can bound the SNR of the selective-transmit-receive diversity system by finding

$$\gamma_{\mathrm{bound}} = \max_{S(\widetilde{H})} \left(\sum_i \widetilde{\lambda}_i^2 \right) = \max_{S(\widetilde{H})} \left(\sum_i \sum_j |\widetilde{h}_{ij}|^2 \right). \tag{3}$$

We note here also that the antenna combination that gives the maximum $\sum_i \widetilde{\lambda}_i^2$ is not necessarily the antenna combination that gives the maximum $\max_i(\widetilde{\lambda}_i^2)$.[3] Nonetheless, the bounds of (2) remain valid when the maximization over all antenna combinations is applied to them.

Now, the maximization in (3) can also be interpreted as being performed over various combinations of L_{t} out of N_{t} columns, whereas the rows of the matrix always have dimension N_{r}. Thus, $\gamma_i = \sum_{j=1}^{N_{\mathrm{r}}} |\widetilde{h}_{ji}|^2$ are (henceforth normalized) chi-square distributed random variables with $2N_{\mathrm{r}}$ degrees of freedom. Note that the γ_i can be interpreted as the received SNR when only the ith antenna is transmitting, and the receiver uses MRC. The joint statistics of the *ordered* SNRs $\gamma_{(i)}$ can be shown to be [11]

$$p_{\gamma(i)}\left(\gamma_{(1)}, \gamma_{(2)}, \ldots, \gamma_{(N_{\mathrm{t}})}\right) = \begin{cases} N_{\mathrm{t}}! \prod_{i=1}^{N_t} \frac{1}{\Gamma(N_{\mathrm{r}})} \gamma_{(i)}^{N_{\mathrm{r}}-1} \\ \qquad \times \exp\left(-\gamma_{(i)}\right), & \text{for } \gamma_{(1)} > \gamma_{(2)} > \ldots \gamma_{(N_{\mathrm{t}})} \\ 0, & \text{otherwise} \end{cases} \tag{4}$$

where $\Gamma(\cdot)$ is the Euler Gamma Function. We utilize L_{t} out of N_{t} variables $\gamma_{(i)}$ and choose the combination that gives maximum SNR. The desired γ_{bound} can be easily written in terms of the ordered SNRs as

$$\gamma_{\mathrm{bound}} = \sum_{i=1}^{L_{\mathrm{t}}} \gamma_{(i)}. \tag{5}$$

B. Statistics of the SNR

The statistics of γ_{bound} can be derived from (4) and (5). Mathematically, this problem is equivalent to deriving the SNR for H-S/MRT with a single receive antenna but with Nakagami channel statistics.[4] Consequently, the simple and elegant techniques for analyzing H-S/MRC with single-transmit-antenna in Rayleigh fading channels [19] can no longer be used. On the other hand, the available techniques for H-S/MRC in Nakagami-fading [12], [20], while mathematically elegant, do not lend themselves easily to computer implementation. We propose a new approach that also exploits the fact that in our case, the degrees of freedom (i.e., the number of antenna elements) can only take on integer values.

Since we are computing the sum of random variables, computing the characteristic function suggests itself naturally. We can write it as

$$\begin{aligned} \Phi(j\nu) = \frac{N_{\mathrm{t}}!}{[\Gamma(N_{\mathrm{r}})]^{N_{\mathrm{t}}}} & \int_0^{\infty} d\gamma_{(1)} \gamma_{(1)}^{N_{\mathrm{r}}-1} e^{-\gamma_{(1)}} e^{-j\nu\Xi(L_{\mathrm{t}}-1)\gamma_{(1)}} \\ & \times \int_0^{\gamma_{(1)}} d\gamma_{(2)} \gamma_{(2)}^{N_{\mathrm{r}}-1} e^{-\gamma_{(2)}} e^{-j\nu\Xi(L_{\mathrm{t}}-2)\gamma_{(2)}} \ldots \\ & \times \int_0^{\gamma_{(N_{\mathrm{t}}-1)}} d\gamma_{(N_{\mathrm{t}})} \gamma_{(N_{\mathrm{t}})}^{N_{\mathrm{r}}-1} e^{-\gamma_{(N_{\mathrm{t}})}} e^{-j\nu\Xi(L_{\mathrm{t}}-N_{\mathrm{t}})\gamma_{(N_{\mathrm{t}})}} \end{aligned} \tag{6}$$

where $\Xi(x)$ is the Heaviside step function

$$\Xi(x) = \begin{cases} 1, & \text{if } x \geq 0 \\ 0, & \text{otherwise} \end{cases}. \tag{7}$$

In the following, we abbreviate the expression $1 + j\nu\Xi(L_{\mathrm{t}} - i)$ as a_i, dropping the dependence on ν for notational convenience. This multiple integral can be shown to result in a polynomial, whose coefficients can be derived analytically by a finite recursion with N_{t} iteration steps.

The crucial step of our proposed technique is now to recognize that an expression of the form

$$\left(d + \sum_p \exp(-b_p x) \wp(p, x) \right) \tag{8}$$

where $\wp(p, x)$ is a polynomial in x whose coefficients may depend on p, retains its basic structure when integrated between 0 and y. Thus, the first $N_{\mathrm{t}} - 1$ integrations can be written in an iterative fashion.

Specifically, let us write the integrand for the first integration (i.e., $q = 0$) as

$$\gamma_{(N_{\mathrm{t}})}^{N_{\mathrm{r}}-1} \exp\left(-\gamma_{(N_{\mathrm{t}})}\right) I^{(0)} \tag{9}$$

and quite generally denote the result of the qth integration as $I^{(q)}$, where superscript $^{(q)}$ indexes the number of performed integrations. The integral $I^{(q)}$ has the form

$$I^{(q)} = d^{(q)} + \sum_{p=1}^{q} e^{-b_p^{(q)} \gamma_{(N_{\mathrm{t}}-q)}} \sum_{k=0}^{(q-p+1)(N_{\mathrm{r}}-1)} c_{p,k}^{(q)} \gamma_{(N_{\mathrm{t}}-q)}^k \tag{10}$$

with initial condition

$$d^{(0)} = 1 \quad b_p^{(0)} = 0 \quad c_{p,k}^{(0)} = 0. \tag{11}$$

[3]The practical implications of this statement for antenna selection algorithms will be discussed in Section IV.

[4]Note that the normalization in a Nakagami channel is usually different from the one used when MRC of several Rayleigh-fading channels. However, that is a detail that does not influence the mathematical approach to derive the distribution.

We show in the Appendix that the central quantities $d^{(q)}$, $b_p^{(q)}$, and $c_{p,k}^{(q)}$ are given by recursion relations

$$b_p^{(q+1)} = b_p^{(q)} + a_{N_\mathrm{t}-q} \quad \text{for} \quad 1 \le p \le q; \tag{12}$$

$$b_{q+1}^{(q+1)} = a_{N_\mathrm{t}-q} \tag{13}$$

$$\widehat{c}_{p,k}^{(q)} = \begin{cases} c_{p,k-(N_\mathrm{r}-1)}^{(q)}, & \text{for } (q-p+2)(N_\mathrm{r}-1) \\ & \quad \ge k \ge (N_\mathrm{r}-1) \\ 0, & \text{otherwise} \end{cases} \tag{14}$$

$$d^{(q+1)} = d^{(q)} \frac{(N_\mathrm{r}-1)!}{\left(a_{N_\mathrm{t}-q}\right)^{N_\mathrm{r}}} + \sum_{p=1}^{q} \sum_{t=0}^{(q-p+2)(N_\mathrm{r}-1)} \frac{t!\, \widehat{c}_{p,t}^{(q)}}{\left(b_p^{(q+1)}\right)^{t+1}} \tag{15}$$

$$c_{p,k}^{(q+1)} = -\sum_{t=0}^{(q-p+2)(N_\mathrm{r}-1)-k} \frac{\widehat{c}_{p,k+t}^{(q)}}{\left(b_p^{(q+1)}\right)^{t+1}} \frac{(k+t)!}{k!} \tag{16}$$

for $1 \le p \le q$ and

$$c_{p,k}^{(q+1)} = -\frac{d^{(q)}}{\left(b_p^{(q+1)}\right)^{N_\mathrm{r}-k}} \frac{(N_\mathrm{r}-1)!}{k!} \tag{17}$$

for $p = q+1$.

The characteristic function of the γ_bound is finally given as

$$\Phi(j\nu) = \frac{N_\mathrm{t}!}{[\Gamma(N_\mathrm{r})]^{N_\mathrm{t}}} \left[d^{(N_\mathrm{t}-1)} (N_\mathrm{r}-1)! a_1^{-N_\mathrm{r}} + \sum_{p=1}^{N_\mathrm{t}-1} \sum_{t=0}^{(N_\mathrm{t}-p+1)(N_\mathrm{r}-1)} \widehat{c}_{p,t}^{(N_\mathrm{t}-1)} t! \left(b_p^{(N_\mathrm{t})}\right)^{-(t+1)} \right]. \tag{18}$$

Note that this is the characteristic function $\Phi(j\nu)$, where the coefficients $d^{(N_\mathrm{t})}$, $\widehat{c}_{p,t}^{(N_\mathrm{r})}$, and $b_p^{(N_\mathrm{t})}$ depend on $j\nu$.

In principle, an analytic inversion of the characteristic function would be possible, giving the probability density function of the SNR $p_{\gamma_\mathrm{bound}}(\cdot)$ in closed form. However, due to the existence of fast Fourier inversion techniques [21], numerical inversion is convenient and fast.

C. Bit Error Probability

Computation of the bit error probability (BEP) can be done by the classical method of averaging the "instantaneous BEP" (i.e., BEP for a given channel realization) over the statistics of the SNR. For coherent demodulation, this gives

$$P_e = K \int_0^\infty Q(\sqrt{a\gamma}) p_\gamma(\gamma) d\gamma \tag{19}$$

where $Q(\cdot)$ is the Gaussian-Q function as defined in [22], and the constants K and a depend on the modulation format [22].

Having derived the characteristic function (c.f.), it is preferable to relate the error probability in terms of the c.f. Recall that minimum shift keying (MSK) with precoded transmitter and derotation of the signal constellation diagram [23] exhibits the same error probability as binary phase-shift keying (BPSK). Thus, the error probability for MSK and BPSK can be computed as [24], [25]

$$P_e = \frac{1}{\pi} \int_0^{\frac{\pi}{2}} \Phi\left(j \frac{1}{\sin^2(\phi)}\right) d\phi. \tag{20}$$

For $\pi/4$-shifted DQPSK (with Gray coding and differential detection), we obtain [26]

$$P_e = \frac{1}{4\pi} \int_{-\pi}^{\pi} \frac{1-\zeta^2}{1+2\zeta\sin(\phi)+\zeta^2} \times \Phi\left(j \frac{2+\sqrt{2}}{2}\left(1+2\zeta\sin(\phi)+\zeta^2\right)\right) d\phi \tag{21}$$

where

$$\zeta = \sqrt{\frac{2-\sqrt{2}}{2+\sqrt{2}}}. \tag{22}$$

D. Capacity

For a capacity point of view, the whole system between encoder and decoder can be viewed as an effective scalar flat-fading channel characterized by the SNR $\gamma_{\mathrm{H-S/MRC}}$ as defined in (1). The capacity for each channel realization is thus given by

$$C(\gamma_{\mathrm{H-S/MRC}}) = \log_2(1 + \bar{\Gamma}\gamma_{\mathrm{H-S/MRC}}) \tag{23}$$

where $\bar{\Gamma}$ is the average SNR of a single-input single-output (SISO) channel. An upper bound for the capacity is obtained by substituting γ_bound, as computed in Section III-B, for $\gamma_{\mathrm{H-S/MRC}}$ (and similarily for the lower bound). Using standard techniques for functions of one random variable [27], the upper bound for the pdf of the capacity becomes

$$p_C(C) = 2^C \frac{\ln(2)}{\bar{\Gamma}} p_{\gamma_\mathrm{bound}}\left(\frac{(2^C-1)}{\bar{\Gamma}}\right). \tag{24}$$

E. Monte Carlo (MC) Simulations

For the influence of nonidealities, we take refuge to computer simulations. We first generate one realization of a multiple transmit/receive antenna channel transfer matrix. For the i.i.d. case, this is trivial, as the entries are independent complex Gaussian random variables. Correlated entries can be created by multiplying the i.i.d. matrix with a matrix $\underline{A}$ that fulfills $\underline{A}\underline{A}^\dagger = \underline{R}$, where $\underline{R}$ is the desired correlation matrix. We then create submatrices of size $N_\mathrm{r} \times L_\mathrm{t}$ by striking $(N_\mathrm{t} - L_\mathrm{t})$ columns from the channel matrix. For each submatrix, we compute the SNR (corresponding to the square of the largest singular value). Finally, we select the antenna combination (submatrix) that gives the largest SNR and store it. This procedure is repeated N_MC times to give a statistical ensemble.

IV. Results

In this section, we present results from our analysis and discuss the influence of the number of available, and actually chosen, antennas on the system performance. Unless otherwise stated, we

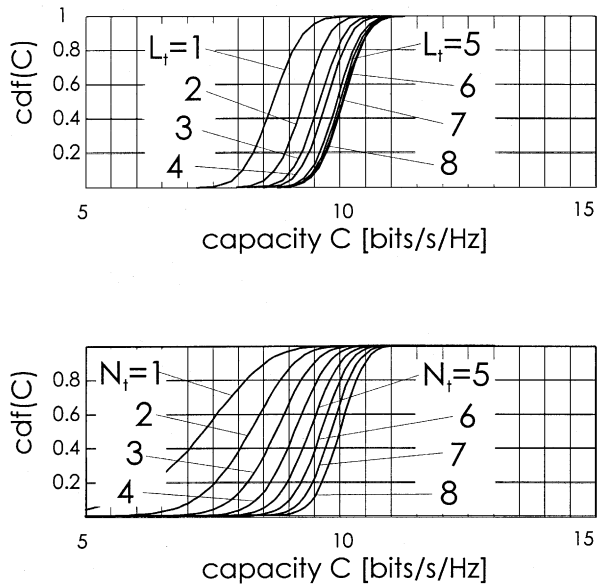

Fig. 2. (Top) Capacity of a system with H-S/MRT at the transmitter and MRC at the receiver for various values of $L_{\rm t}$ with $N_{\rm t} = 8$, $N_{\rm r} = 2$, and SNR= 20 dB. Bottom: Capacity of a system with MRT at transmitter and MRC at receiver for various values of $N_{\rm t}$ and $N_{\rm r} = 2$, SNR= 20 dB.

will use the following system parameters: $\bar{\Gamma} = 20$ dB, $N_{\rm t} = 8$, and $N_{\rm r} = 2$. For the BEP computations, we use minimum shift keying $\pi/4$-DQPSK or MSK since these are commonly used in mobile radio systems.

A. Results in Idealized Environments

Fig. 2 shows the cumulative distribution function (CDF) of the capacity for different values of $L_{\rm t}$ (as obtained from Monte Carlo simulations). We see that the capacity obtained with $L_{\rm t} = 3$ is already very close to the capacity of a full-complexity scheme. We also see that the improvement by going from one to three antennas is larger than the improvement by going from three to eight. For comparison, we also show the capacity with pure MRT. The required number of RF chains is $L_{\rm t}$ for the H-S/MRT case and $N_{\rm t}$ for the pure MRT case. Naturally, the capacity is the same for H-S/MRT with $L_{\rm t} = 8$ and MRT with $N_{\rm t} = 8$. For a smaller number of RF chains, however, the hybrid scheme is much more effective (for the same number of RF chains), both in terms of diversity degree (slope of the curve) and ergodic capacity. This confirms the effectiveness of using H-S/MRT.

Fig. 3 shows the CDF of the capacity for different numbers of selected antennas $L_{\rm t}$. The exact curve was computed by MC simulations, and the upper and lower bounds were computed by the analytical method described in Section III. We note that upper and lower bound are separated by about 1 bit/s/Hz, except for the case $L_{\rm t} = 1$, where they coincide and agree with the exact curve.

Apart from the bounds and the exact curves (computed by MC simulations), we also exhibit the CDF of the capacity when a suboptimum antenna selection criterion is used. This criterion, which we referred to as power selection criterion, works the following way: We transmit from a single antenna $i = 1$ and determine the SNR that can be obtained at the receiver with MRC.

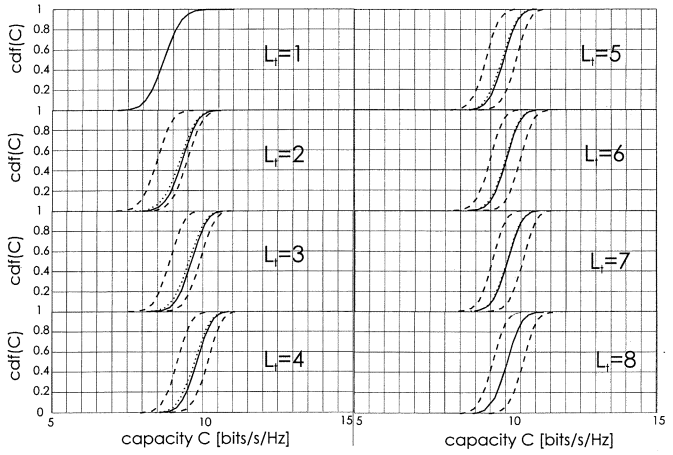

Fig. 3. CDF of the capacity: Lower bound (left dashed curves), upper bound (right dashed curves), exact (solid curves), and exact with the use of the simplified selection criterion (dotted). $N_{\rm t} = 8$, $N_{\rm r} = 2$, SNR= 20 dB.

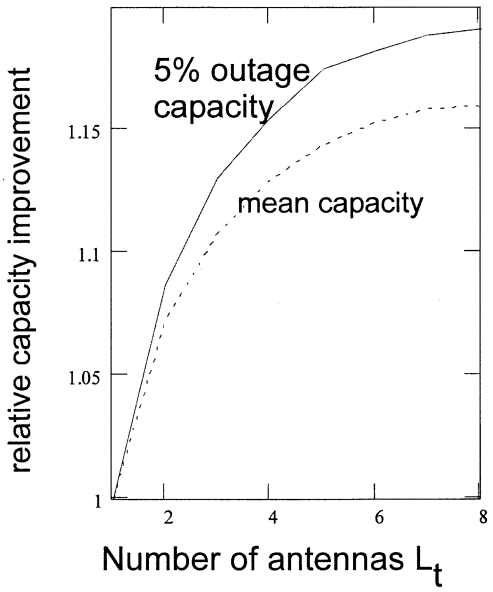

Fig. 4. Capacity increase of the 5% outage capacity and the ergodic capacity compared with $L_{\rm t} = 1$ when having several *active* antennas at the transmitter. $N_{\rm t} = 8$, $N_{\rm r} = 2$, SNR= 20 dB.

Then, we transmit from the next antenna $i = 2$ and determine again the SNR with MRC, and so on. Then, the $L_{\rm t}$ antennas that resulted in the best SNR are chosen. This can also be interpreted as optimizing $\gamma_{\rm bound}$ instead of $\lambda_{\rm max}$. The advantage of this technique is that the determination of the "optimum" antennas is much simpler than if we were to perform a full search among all possible antenna combinations. Furthermore, the loss in performance is less than 0.05 bits/s/Hz. Note that an alternative antenna selection scheme, based on eigenprecoding, was proposed in [28].

Fig. 4 shows the increase of the ergodic capacity and 5% outage capacity as a function of the number of selected antennas. We see that increasing that number from 1 to 2 gives about the same gain as increasing from 2 to 8. It seems thus reasonable to use only two or three selected antennas, resulting in large cost savings with only a small performance loss.

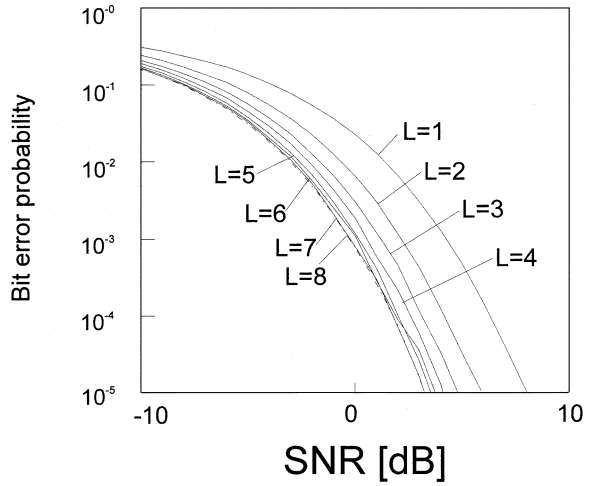

Fig. 5. BEP as a function of SNR for $\pi/4$-DQPSK as modulation format.

Fig. 5 shows the downlink BEP of $\pi/4$-DQPSK as a function of the mean SNR $\bar{\Gamma}$ for a different number of selected antennas $L_{\rm t}$. Again, we observe a big improvement going from $L_{\rm t}=1$ to $L_{\rm t}=3$ (3 dB at a error probability $P_e=10^{-3}$), whereas the gain going from $L_{\rm t}=3$ to $L_{\rm t}=8$ is only an additional 1.5 dB.

Generally, the achieved capacities are much lower than those usually associated with multiple-input-multiple-output (MIMO) systems. The difference is due to the restriction of the possible structures of the transmitter and receiver, allowing for only a single data stream to be transmitted. Specifically, we allow only a scalar coder and distinguish the signals at the different antennas only by linear weights and not by different codes at each antenna. Comparisons with MIMO systems show that with appropriate (space-time) processing and coding, an outage capacity of 16 bits/s/Hz is possible for $L_{\rm t}=8$, $N_{\rm r}=2$ [29]. The difference with the 10 bits/s/Hz obtained with the linear system is the price for backward compatibility and greater simplicity. We also note that the increase in capacity slows down as we increase $L_{\rm t}$ but shows no sharp discontinuity as $L_{\rm t}$ increases beyond $N_{\rm r}=2$. This is due to the fact that we use linear transmitters and receivers so that every gain in SNR readily translates into a gain in capacity.

B. Effect of Nonidealities

Fig. 6 shows the influence of correlation between the transmit antenna elements on the performance of the hybrid system. We show the 10% outage capacity of a 3/8 system (i.e., $L_{\rm t}=3$, $N_{\rm t}=8$, with two receive antennas)

i) for optimum selection of the transmit antennas (i.e., choosing the transmit antennas that give the best SNR);
ii) with power selection of the transmit antennas as desribed above;
iii) with MRT with $N_{\rm t}=8$.

The outage capacity is plotted as a function of the ratio of correlation length of the channel to antenna spacing. We observe that the relative performance loss due to correlation is higher for the 3/8 system than for the 8/8 system. This can be explained by the fact that in a highly correlated channel, no diversity gain can be achieved, but all gain is due to beamforming. Thus antenna selection is ineffective, and the (beamforming) gain is only influenced by the number of actually used antenna elements. We furthermore observe that the difference between the power selection criterion and optimum antenna selection decreases as the correlation between the antennas increases and vanishes at very large correlations. This makes sense, as the difference between the chosen antenna signals vanishes for highly correlated signals.

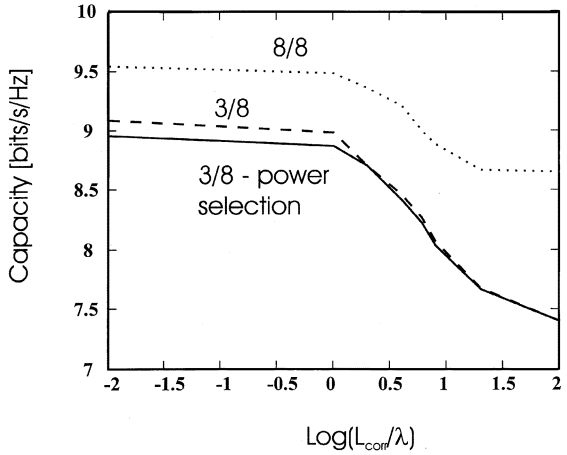

Fig. 6. Ten percent outage capacity of a system with two receiver antennas and H-S/MRT at the transmitter as a function of the antenna spacing. Dashed: 3/8 system with optimum antenna selection. Solid: 3/8 system with power selection criterion. Dotted: 8/8 system. Corrected coefficient between signals at two antenna elements that are spced d apart is $\exp(-d/L_{\rm corr}$.

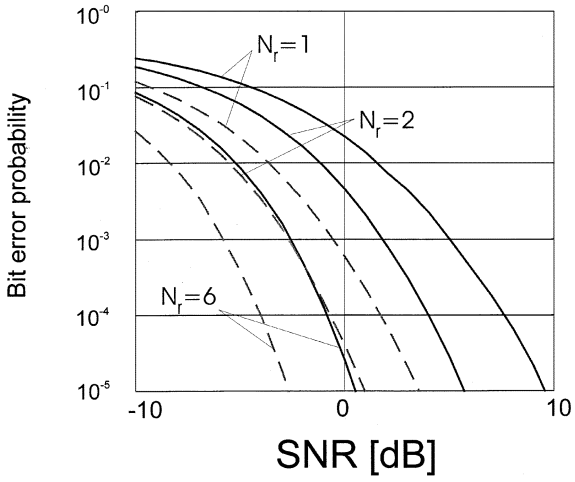

Fig. 7. Influence of the number of receive antennas on the BEP. MSK modulation: 8/8 (solid) and 1/8 (dashed) H-S/MRT at transmitter.

Fig. 7 shows the influence of the number of antenna elements at the receiver. We find that as the number of receive antennas increases, the advantage of going from a 1/8 to an 8/8 system at the transmitter decreases. This is intuitively clear, as the beneficial effect of selecting more antennas is smaller if there are already a lot of diversity antennas.

We have also investigated the influence of erroneous antenna selection on the capacity of the system. We assume that in a first stage, the complete channel transfer matrix is estimated. Based on that measurement, the antennas that are used for the

actual data transmission are selected, and the antenna weights are determined. We distinguish four different cases:

i) perfect choice of the antennas and the antenna weights;
ii) imperfect antenna selection but perfect antenna weights (this can be achieved by measuring the transfer function of the actually selected antennas with a longer training sequence);
iii) imperfect choice of the antennas, as well as of the antenna weights at the transmitter, and perfect antenna weights at the receiver (this is plausible if the feedback is done with finite precision and a finite lag);
iv) imperfect choice of the antenna weights at transmitter and receiver.

The errors in the transfer functions are assumed to have a complex Gaussian distribution with $\mathrm{SNR}_{\mathrm{pilot}}$, which is the SNR during the transmission of the pilot tones. We found that measurement with an $\mathrm{SNR}_{\mathrm{pilot}}$ of 10 dB results in a still tolerable loss of capacity (less than 5%). However, below that level, the capacity starts to decrease significantly. This is shown in Fig. 8.

V. Results in Measured Channels

We have also investigated the performance of our proposed scheme in measured channels. The measurements took place in a microcellular environment, specifically in a courtyard in Ilmenau, Germany. Four different measurement scenarios have been analyzed, and full details of the measurement scenarios can be found in [30]. For clarity, only two scenarios are presented here, and they are as follows:[5]

Scenario I: Closed back-yard of size 34×40 m with inclined rectangular extension. The receiver array is situated in one rectangular corner with the array broad side pointing under 45° inclination directly to the middle of the back yard. The LOS connection between the transmitter and the receiver is 28 m.

Scenario II: Same back yard as in Scenario I but with artificially obstructed LOS path. It is expected that the metallic objects generate serious multipath and high-order scattering that can only be observed within the dynamic range of the measurement system if the strong LOS path is obstructed.

The main features of the measured channels are the following.

i) The number of multipath components with significant amplitude is limited. Using high-resolution algorithms, we found between 20 and 40 multipath components.
ii) The angular spectrum of the arriving waves deviates from a uniform spectrum; the angular spread at the receiver is limited by the opening angle of the used antenna to less than 120°.
iii) The LOS component in Scenario I leads to a higher correlation between the signals.

In order to determine distributions of channel capacity and eigenvalues, a large number of measurements are required, which means a large effort. Thus, for the measured channels, we evaluate the different distributions by a method introduced in [31] in order to keep the number of required measurements to a reasonable number. In this method we first measure the double directional impulse response, i.e., direction of departure, direc-

[5]Scenarios I and II correspond to scenarios II and III in [30], respectively.

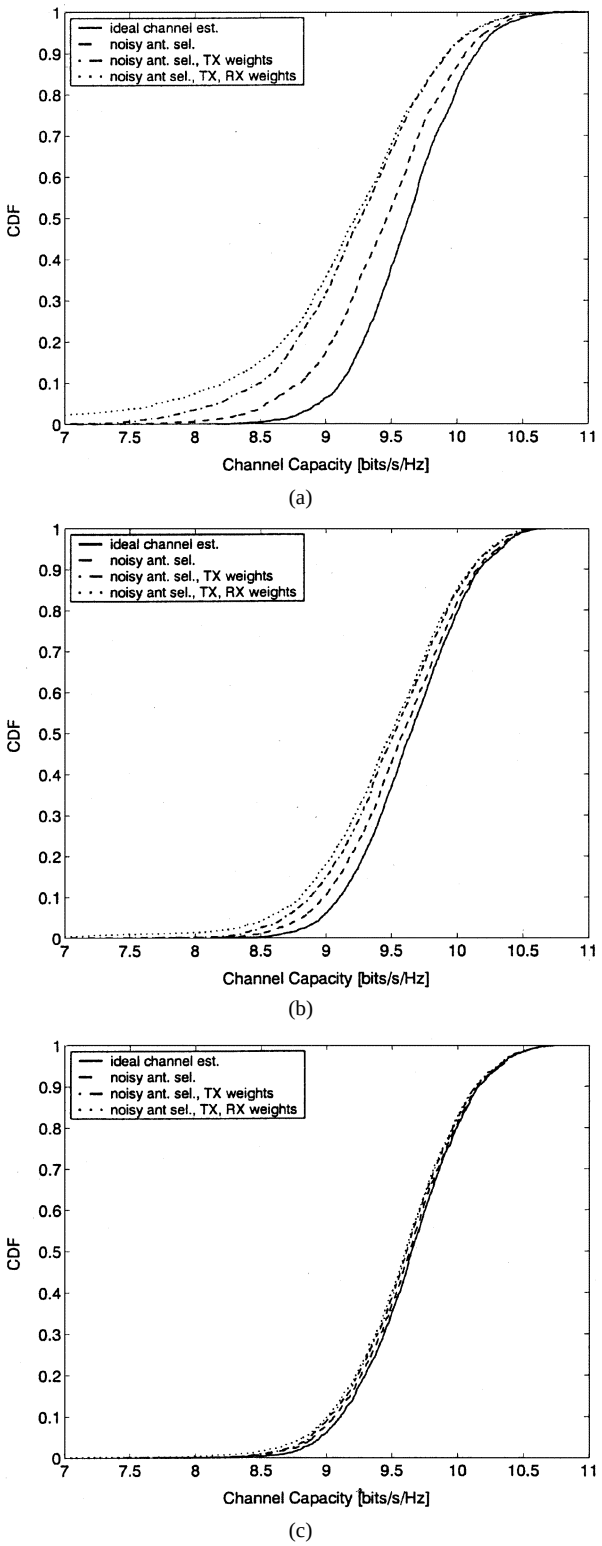

Fig. 8. Impact of errors in the estimation of transfer function matrix H. CDF of the capacity for i) ideal channel knowledge at TX and RX (solid), ii) imperfect antenna selection but perfect antenna weights (dashed), iii) imperfect antenna weights at TX only (dotted), and iv) imperfect antenna weights at TX and RX (dash-dotted). (a) $\mathrm{SNR}_{\mathrm{pilot}} = 5$ dB. (b) $\mathrm{SNR}_{\mathrm{pilot}} = 10$ dB. (c) $\mathrm{SNR}_{\mathrm{pilot}} = 15$ dB.

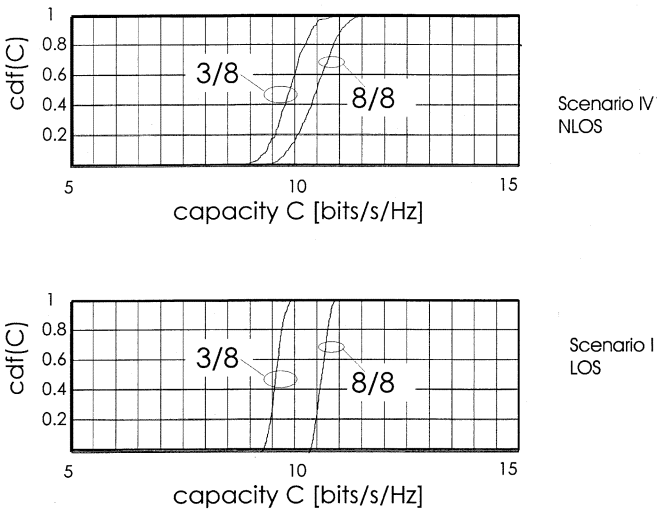

Fig. 9. Capacity of H-S/MRT system with $L_{\rm t}=3$ and $N_{\rm t}=8$ elements and an MRT system with $N_{\rm t}=8$ elements in a microcellular environment. The number of receive antennas is $N_{\rm r}=2$. See text for description of the scenarios.

tion of arrival, time delay, and power of the different taps. Then several impulse responses are *synthetically* generated from these measurements by assigning independent uniformly distributed $[0,2\pi]$ random phases α_k to the different realizations of $h_{m,n}$ as

$$h_{m,n}=\sum_{k=1}^{K}A_k e^{j\phi_k}e^{-j\frac{2\pi}{\lambda}d(m\sin(\Omega_{{\rm R},k})+n\sin(\Omega_{{\rm T},k}))}e^{j\alpha_k} \quad (25)$$

where m and n index the antenna elements, K is the number of multipath components, A_k and ϕ_k is the magnitude and phase of the kth multipath component, and $\Omega_{{\rm R},k}$ and $\Omega_{{\rm T},k}$ are the angle between the multipath component and the receive- and transmit array, respectively. The α_k stay unchanged as the different antenna elements are considered.

Fig. 9 shows plots of the capacity for a 3/8 H-S/MRT system and an eight-element MRT scheme. The number of receive antennas in both cases is $N_{\rm r}=2$. We see that the performance that can be achieved in that environment is very close to the performance in i.i.d. channels.

VI. Summary and Conclusions

We have investigated reduced-complexity wireless systems with transmit and receive diversity. The complexity reduction is achieved by using H-S/MRT on one link end and MRC at the other. We note that for MRT and H-S/MRC, the results are equally applicable. Since the transceiver structure employs only weighted versions of the same signals, such a system is fully compatible with existing mobile radio systems, whereas the use of multiple antennas at both transmitter and receiver results in a high degree of diversity. The H-S/MRT(C) offers advantages when a large number of transmit antennas and a limited number of RF chains are available. By choosing the best $L_{\rm t}$ out of $N_{\rm t}$ antennas, little signal quality is lost compared with the full-complexity version, while drastically reducing the involved hardware expenses. We have seen that for a practically useful example ($N_{\rm t}=8$, $N_{\rm r}=2$, SNR$=$ 20 dB), $L_{\rm t}=2$ to 3 is a good compromise between hardware expense and performance.

In summary, we find that a reduced-complexity multiple transmit/receive antenna system can bring remarkable improvement in the transmission quality of existing systems while requiring only moderate hardware expenses and keeping backward compatibility. For a system that is to be designed from scratch, on the other hand, the use of space time coding instead of a linear transceiver structures would offer advantages both from a capacity point of view and from the fact that it can also be easily applied to FDD systems since channel knowledge at the transmitter is not required.

Appendix
Derivation of the Recursion Relation

The starting point is (10) combined with (6)

$$\int_0^y\left[d^{(q)}+\sum_{p=1}^{q}\exp\left(-b_p^{(q)}x\right)\sum_{k=0}^{(q-p+1)(N_{\rm r}-1)}c_{p,k}^{(q)}x^k\right]\times x^{N_{\rm r}-1}\exp\left(-xa_{N_{\rm t}-q}\right)dx \quad (26)$$

where for easier readability, we have substituted $\gamma_{N{\rm t}-q}\rightarrow x$, $\gamma_{N{\rm t}-q-1}\rightarrow y$.

The first term of the integral (26) can be solved as [32]

$$\int_0^y d^{(q)}x^{N_{\rm r}-1}\exp\left(-xa_{N_{\rm t}-q}\right)dx=d^{(q)}\left[\frac{1}{a_{N_{\rm t}-q}^{N_{\rm r}}}(N_{\rm r}-1)!-\frac{\exp\left(-a_{N_{\rm t}-q}y\right)}{a_{N_{\rm t}-q}^{N_{\rm r}}}\sum_{k=0}^{N_{\rm r}-1}\frac{(N_{\rm r}-1)!}{k!}a_{N_{\rm t}-q}^{k}y^k\right]. \quad (27)$$

Next, we pull out from the integral sign the summation over p and consider the pth term in the basic integral (26)

$$J_p^{(q)}=\int_0^y\left[\exp\left(-b_p^{(q)}x\right)\sum_{k=0}^{(q-p+1)(N_{\rm r}-1)}c_{p,k}^{(q)}x^k\right]\times x^{N_{\rm r}-1}\exp\left(-xa_{N_{\rm t}-q}\right)dx. \quad (28)$$

By introducing

$$\widehat{b}_p^{(q)}=b_p^{(q)}+a_{N_{\rm t}-q}\ \text{for}\ 1\le p\le q \quad (29)$$

$$\widehat{b}_{q+1}^{(q)}=a_{N_{\rm t}-q} \quad (30)$$

$$M=(q-p+2)(N_{\rm r}-1) \quad (31)$$

$$\widehat{c}_{p,k}^{(q)}=\begin{cases}c_{p,k-(N_{\rm r}-1)}^{(q)}, & \text{for } (q-p+2)(N_{\rm r}-1)\\ & \quad\ge k\ge(N_{\rm r}-1)\\ 0, & \text{otherwise}\end{cases} \quad (32)$$

this integral can be written as

$$J_p^{(q)}=\int_0^y\exp\left(-\widehat{b}_p^{(q)}x\right)\sum_{k=0}^{M}\widehat{c}_{p,k}^{(q)}x^k dx. \quad (33)$$

Employing [33]

$$\int\sum_{k=0}^{M}\widehat{c}_{p,k}^{(q)}x^k e^{-\widehat{b}_p^{(q)}x}dx=\frac{e^{-\widehat{b}_p^{(q)}x}}{-\widehat{b}_p^{(q)}}\sum_{l=0}^{M}\frac{(-1)^l}{\left(-\widehat{b}_p^{(q)}\right)^l}\frac{d^l}{dx^l}\sum_{k=0}^{M}\widehat{c}_{p,k}^{(q)}x^k \quad (34)$$

we get

$$J_p^{(q)} = \left. \frac{e^{-\widehat{b}_p^{(q)}x}}{-\widehat{b}_p^{(q)}} \sum_{l=0}^{M} \frac{(-1)^l}{\left(-\widehat{b}_p^{(q)}\right)^l} \sum_{k=0}^{M} \widehat{c}_{p,k}^{(q)} \frac{d^l}{dx^l} x^k \right|_0^y$$

$$= \left. \frac{e^{-\widehat{b}_p^{(q)}x}}{-\widehat{b}_p^{(q)}} \sum_{k=0}^{M} \widehat{c}_{p,k}^{(q)} \sum_{l=0}^{k} \frac{1}{\left(\widehat{b}_p^{(q)}\right)^l} \frac{k!}{(k-l)!} x^{k-l} \right|_0^y. \quad (35)$$

Introducing $r = k - l$, we can write this as

$$J_p^{(q)} = \left. -\frac{e^{-\widehat{b}_p^{(q)}x}}{\widehat{b}_p^{(q)}} \sum_{r=0}^{M} x^r \sum_{t=0}^{M-r} \widehat{c}_{p,r+t}^{(q)} \frac{1}{\left(\widehat{b}_p^{(q)}\right)^t} \frac{(r+t)!}{r!} \right|_0^y.$$

The total integral thus is

$$d^{(q)} \left[\frac{1}{\left(\widehat{b}_{q+1}^{(q)}\right)^{N_\mathrm{r}}} (N_\mathrm{r}-1)! - \frac{\exp\left(-\widehat{b}_{q+1}^{(q)} y\right)}{\left(\widehat{b}_{q+1}^{(q)}\right)^{N_\mathrm{r}}} \times \sum_{k=0}^{N_\mathrm{r}-1} \frac{(N_\mathrm{r}-1)!}{k!} \left(\widehat{b}_{q+1}^{(q)}\right)^k y^k \right]$$

$$+ \sum_{p=1}^{q} \left[\frac{1}{\widehat{b}_p^{(q)}} \sum_{t=0}^{M} \widehat{c}_{p,t}^{(q)} \frac{t!}{\left(\widehat{b}_p^{(q)}\right)^t} - \frac{e^{-\widehat{b}_p^{(q)}y}}{\widehat{b}_p^{(q)}} \times \sum_{r=0}^{M} y^r \sum_{t=0}^{M-r} \widehat{c}_{p,r+t}^{(q)} \frac{1}{\left(\widehat{b}_p^{(q)}\right)^t} \frac{(r+t)!}{r!} \right]. \quad (36)$$

Comparing this expression with the generic expression for the result of the $q+1$th integration

$$\left[d^{(q+1)} + \sum_{p=1}^{q+1} \exp\left(-b_p^{(q+1)} y\right) \sum_{k=0}^{(q-p+2)(N_\mathrm{r}-1)} c_{p,k}^{(q+1)} y^k \right] \quad (37)$$

and matching coefficients, we get the recursion relations (12)–(16) given in Section III-B.

For the last integration, we use the fact that [33]

$$\int_0^\infty x^k \exp(-ax) dx = k! a^{-k-1} \quad (38)$$

so that

$$\int_0^\infty \left[d^{(q)} + \sum_{p=1}^{N_t-1} \exp\left(-b_p^{(N_t-1)} x\right) \sum_{k=0}^{(N_t-p)(N_\mathrm{r}-1)} c_{p,k}^{(N_t-1)} x^k \right] \times x^{N_\mathrm{r}-1} \exp\left(-x a_1\right) dx$$

$$= d^{(N_\mathrm{t}-1)} \frac{(N_\mathrm{r}-1)!}{a_1^{N_\mathrm{r}}} + \sum_{p=1}^{N_\mathrm{t}-1} \left[\sum_{t=0}^{(N_\mathrm{t}-p+1)(N_\mathrm{r}-1)} \widehat{c}_{p,t}^{(N_\mathrm{t}-1)} \frac{t!}{\left(b_p^{(N_\mathrm{t})}\right)^{t+1}} \right]. \quad (39)$$

REFERENCES

[1] J. H. Winters, "On the capacity of radio communications systems with diversity in Rayleigh fading environments," *IEEE J. Select. Areas Commun.*, vol. JSAC-5, pp. 871–878, June 1987.

[2] G. J. Foschini and M. J. Gans, "On limits of wireless communications in fading environments when using multiple antennas," *Wireless Pers. Commun.*, vol. 6, pp. 311–335, 1998.

[3] G. J. Foschini, "Layered space-time architecture for wireless communication in a fading environment when using multi-element antennas," *Bell Labs Tech. J.*, pp. 41–59, Autumn 1996.

[4] G. J. Foschini, G. D. Golden, R. A. Valenzuela, and P. W. Wolniansky, "Simplified processing for high spectral efficiency wireless communication employing multi-element arrays," *IEEE J. Select. Areas Commun.*, vol. 17, pp. 1841–1852, Nov. 1999.

[5] A. Wittneben, "A new bandwidth efficient transmit antenna modulation diversity scheme for linear digital modulation," in *Proc. IEEE Int. Conf. Commun.*, Geneva, Switzerland, 1993, pp. 1630–1634.

[6] J. H. Winters, "The diversity gain of transmit diversity in wireless systems with rayleigh fading," in *Proc. IEEE Int. Conf. Commun.*, Piscataway, NJ, 1994, pp. 1121–1125.

[7] T. K. Y. Lo, "Maximum ratio transmission," in *Proc. IEEE Int. Conf. Commun.*, Piscataway, NJ, 1999, pp. 1310–1314.

[8] J. B. Andersen, "Antenna arrays in mobile communications: gain, diversity, and channel capacity," *IEEE Antennas Propagat. Mag.*, vol. 42, pp. 12–16, Apr. 2000.

[9] N. Kong and L. B. Milstein, "Combined average SNR of a generalized diversity selection combining scheme," in *Proc. IEEE Int. Conf. Commun.*, vol. 3, Atlanta, GA, June 1998, pp. 1556–1560.

[10] M. Z. Win and J. H. Winters, "Analysis of hybrid selection/maximal-ratio combining of diversity branches with unequal SNR in Rayleigh fading," in *Proc. 49th Annu. Int. Veh. Technol. Conf.*, 1, Houston, TX, May 1999, pp. 215–220.

[11] ——, "Virtual branch analysis of symbol error probability for hybrid selection/maximal-ratio combining in Rayleigh fading," *IEEE Trans. Commun.*, vol. 49, pp. 1926–1934, Nov. 2001.

[12] M. S. Alouini and M. K. Simon, "Performance of coherent receivers with hybrid SC/MRC over Nakagami-m fading channels," *IEEE Trans. Veh. Technol.*, vol. 48, pp. 1155–1164, July 1999.

[13] R. K. Mallik and M. Z. Win, "Analysis of hybrid selection/maximal-ratio combining in correlated Nakagami fading," *IEEE Trans. Commun.*, pp. 1372–1383, Aug. 2002.

[14] S. Thoen, L. V. der Perre, M. Engels, and B. Gyselinckx, "Performance analysis of combined transmit-SC/receive-MRC," *IEEE Trans. Commun.*, vol. 49, pp. 5–8, Jan. 2001.

[15] E. T. S. I. (ETSI), Radio equipment and systems: European cordless telecommunications standard interface, in DECT Specs., , vol. part 1–3, version 02.01, 1991.

[16] J. Gibson, *The Mobile Radio Handbook*. New York: IEEE, 1996.

[17] T. S. Rappaport, *Wireless Communications Principles and Practice*. New York: IEEE, 1996.

[18] R. A. Horn and C. R. Johnson, *Matrix Analysis*. Cambridge, U.K.: Cambridge Univ. Press, 1985.

[19] M. Z. Win and J. H. Winters, "Analysis of hybrid selection/maximal-ratio combining in Rayleigh fading," *IEEE Trans. Commun.*, vol. 47, pp. 1773–1776, Dec. 1999.

[20] M. S. Alouini and M. K. Simon, "Application of the dirichlet transformation to the performance evaluation of generalized selection bomining over Nakagami-m fading channels," *J. Commun. Networks*, vol. 1, pp. 5–13, 1999.

[21] W. H. Press *et al.*, *Numerical Recipes*. Cambridge, U.K.: Cambridge Univ. Press, 1996.

[22] J. G. Proakis, *Digital Communications*, 3rd ed. New York: McGraw-Hill, 1995.

[23] G. L. Stuber, *Principles of Mobile Communications*, Second ed. Boston, MA: Kluwer, 2001.

[24] C. Tellambura, A. J. Mueller, and V. K. Bhargawa, "Analysis of m-ary phase-shift keying with diversity reception for land-mobile satellite channels," *IEEE Trans. Veh. Technol.*, vol. 46, pp. 910–922, Nov. 1997.

[25] M. Z. Win, G. Chrisikos, and N. R. Sollenberger, "Performance of rake reception in dense multipath channels: implications of spreading bandwidth and selection diversity order," *IEEE J. Select. Areas Commun.*, to be published.

[26] M. K. Simon and M.-S. Alouini, "A unified approach to the performance analysis of digital communication over generalized fading channels," *Proc. IEEE*, vol. 86, pp. 1858–1877, Sept. 1998.
[27] A. Papoulis, *Probability, Random Variables, and Stochastic Processes*. Tokyo, Japan: McGraw Hill, 1965.
[28] R. Inner and G. Fettweis, "Combined transmitter and receiver optimization for multiple-antenna frequency-selective channels," in *Proc. 5th Int. Symp. Wireless Personal Multimedia Commun.*, 2002, pp. 412–416.
[29] A. F. Molisch, M. Z. Win, and J. H. Winters, "Capacity of MIMO systems with antenna selection," in *Proc. IEEE Int. Conf. Commun.*, Helsinki, Finland, 2001, pp. 570–574.
[30] M. Steinbauer, A. F. Molisch, and E. Bonek, "The double-directional radio channel," *IEEE Antennas Propagat. Mag.*, vol. 43, pp. 51–63, Aug. 2001.
[31] A. F. Molisch, M. Steinbauer, M. Toeltsch, E. Bonek, and R. Thoma, "Capacity of MIMO systems based on measured wireless channels," *IEEE J. Select. Areas Commun.*, vol. 20, pp. 561–569, Apr. 2002.
[32] M. Abramowitz and I. A. Stegun, *Handbook of Mathematical Functions*. New York: Dover, 1965.
[33] I. S. Gradshteyn and I. M. Ryzhik, *Table of Integrals, Series, and Products*. New York: Academic, 1994.

Andreas F. Molisch (S'89–M'95–SM'00) received the Dipl. Ing., Dr. techn., and habilitation degrees from the Technical University Vienna (TU Vienna), Vienna, Austria, in 1990, 1994, and 1999, respectively.

From 1991 to 2000, he was with the TU Vienna, where he became an associate professor in 1999. From 2000 to 2002, he was with the Wireless Systems Research Department, AT&T Laboratories Research, Middletown, NJ. Since then, he has been a Senior Principal Member of Technical Staff with Mitsubishi Electric Research Labs, Cambridge, MA. He is also professor and chairholder for radio systems at Lund University, Lund, Sweden. He has done research in the areas of SAW filters, radiative transfer in atomic vapors, atomic line filters, smart antennas, and wideband systems. His current research interests are MIMO systems, measurement and modeling of mobile radio channels, and UWB. He has authored, co-authored, or edited two books, six book chapters, some 60 journal papers, and numerous conference contributions. He was co-editor of a recent special issue on MIMO and smart antennas in the *J. Wireless Communications and Mobile Computing*.

Dr. Molisch is an editor of the IEEE TRANSACTIONS ON WIRELESS COMMUNICATIONS. He has participated in the European research initiatives "COST 231," "COST 259," and "COST273," where he is chairman of the MIMO channel working group. He is also vice chairman of Commission C (signals and systems) of the International Union of Radio Scientists and is the recipient of several awards.

Moe Z. Win (S'85–M'87–SM'97) received the B.S. degree (magna cum laude) from Texas A&M University, College Station, and the M.S. degree from the University of Southern California (USC), Los Angeles, in 1987 and 1989, respectively, in electrical engineering. As a Presidential Fellow at USC, he received both the M.S. degree in applied mathematics and the Ph.D. degree in electrical engineering in 1998. He is a Distinguished Alumnus of Mountain View College, Dallas, TX.

In 1987, he joined the Jet Propulsion Laboratory (JPL), California Institute of Technology, Pasadena, where he performed research on digital communications and optical systems for NASA space exploration missions. From 1994 to 1997, he was a Research Assistant with the Communication Sciences Institute at USC, where he played a key role in the successful creation of the Ultra-Wideband Radio Laboratory. From 1998 to 2002, he was with the Wireless Systems Research Department, AT&T Laboratories-Research, Middletown, NJ. Since 2002, he has been with the Laboratory for Information and Decision Systems (LIDS), Massachusetts Institute of Technology, Cambridge, where he holds the Charles Stark Draper Chair. His main research interests are the application of mathematical and statistical theories to communication, detection, and estimation problems, including measurement of modeling of time-varying channels, design and analysis of multiple antenna systems, ultra-wide bandwidth (UWB) communications systems, optical communications systems, abd space communications systems.

Dr. Win has been involved actively in organizing and chairing sessions and has served as a member of the Technical Program Committee in a number of international conferences. He currently serves as the Technical Program Chair for the IEEE Communication Theory Symposium of ICC-2004. He served as the Technical Program Chair for the IEEE Communication Theory Symposium of Globecom-2000 and the IEEE International Conference on Ultra Wideband Systems and Technologies in 2002, Technical Program Vice-Chair for the IEEE International Conference on Communications in 2002, and the Tutorial Chair for the IEEE Semiannual International Vehicular Technology Conference in Fall 2001. He is the secretary of the Radio Communications Technical Committee, the current Editor for equalization and diversity for the IEEE TRANSACTIONS ON COMMUNICATIONS, and a Guest-Editor for the 2002 IEEE JOURNAL ON SELECTED AREAS IN COMMUNICATIONS, Special Issue on Ultra-Wideband Radio in Multiaccess Wireless Communications. He received the IEEE Communications Society Best Student Paper Award at the Fourth Annual IEEE NetWorld+Interop'97 Conference in 1997, the International Telecommunications Innovation Award from the Korea Electronics Technology Institute in 2002, a Young Investigator Award from the Office of Naval Research in 2003, and the IEEE Antennas and Propagation Society Sergei A. Schelkunoff Transactions Prize Paper Award in 2003.

Jack H. Winters (S'77–M'81–SM'88–F'96) received the B.S.E.E. degree from the University of Cincinnati, Cincinnati, OH, in 1977 and the M.S. and Ph.D. degrees in electrical engineering from The Ohio State University, Columbus, in 1978 and 1981, respectively.

In 1981, he joined AT&T Bell Laboratories, Middletown, NJ, where he was in the research area for more than 20 years. At AT&T, he was Division Manager of the Wireless Systems Research Division of AT&T Labs-Research. His research interests include signal processing techniques for increasing the capacity and reducing signal distortion in fiber optic, mobile radio, and indoor radio systems and currently studying equalization, smart antennas, and adaptive arrays for cellular systems and wireless local area networks. He is currently consulting for several wireless and optical communication companies.

Dr. Winters is an IEEE Distinguished Lecturer for both the IEEE Communications and the Vehicular Technology Societies, Area Editor for Transmission Systems for the IEEE TRANSACTIONS ON COMMUNICATIONS, and was New Jersey Inventor of the Year for 2001.